International Journal of Technology 12(3) 527-538 (2021)
Received January 2021 / Revised February 2021 / Accepted April 2021

International Journal of Technology

http://ijtech.eng.ui.ac.id

Experimental and Numerical Investigation into the Effect of the Axe-Bow on the Drag Reduction of a Trimaran Configuration

I Ketut Aria Pria Utama[1*], Sutiyo[2], Ketut Suastika[1]

[1]*Department of Naval Architecture, Faculty of Marine Technology, Institut Teknologi Sepuluh Nopember, Kampus ITS Sukolilo, Surabaya 60111, Indonesia*
[2]*Department of Naval Architecture, Faculty of Engineering and Marine Science, University of Hang Tuah, Jalan Arief Rahman Hakim 150, Surabaya 60111, Indonesia*
[1]*Department of Naval Architecture, Faculty of Marine Technology, Institut Teknologi Sepuluh Nopember, Kampus ITS Sukolilo, Surabaya 60111, Indonesia*

Abstract. Using the axe-bow to reduce total ship resistance on monohull ships has been well-known. This advantage has been further applied to a trimaran configuration together with its space-to-length (S/L) ratio differences. The investigation was carried out experimentally using an ITTC standard towing tank and numerically using computational fluid dynamics (CFD) analysis. The base model for the study uses an NPL 4a both for the mainhull and sidehulls of the trimaran, and later the mainhull is modified by attaching a front bulb known as an axe-bow. The resistance analysis of the trimaran was conducted with and without an axe-bow on the mainhull together with S/L ratios of S/L = 0.3 and S/L = 0.4 and at various Froude (Fr) numbers: 0.15, 0.2, 0.25, 0.3, 0.4, and 0.5. The results showed that the monohull with an axe-bow had a smaller drag than that without an axe-bow of an order up to 11.5%, whereas in the trimaran form, the reduction of drag was up to 8.4%. This indicates a positive influence of using the axe-bow on the total resistance of the trimaran configuration. Both experimental and CFD methods showed positive agreement of the order 2.7% discrepancy for the monohull form and a 3.4% discrepancy for the trimaran configuration.

Keywords: Axe-Bow; CFD; Experiment; NPL; Resistance; Trimaran

1. Introduction

There is increased interest in trimaran vessels due to their advantages and applications (Elcin, 2003). The trimaran has sidehulls for gaining ship stability. Three hulls make the trimaran completely unsinkable. Even in the roughest weather, the ultimate hazard of capsizing is minimized. Mainhulls and sidehulls can be modified flexibly to reduce resistance (Sulistyawati and Suranto, 2020). Therefore, the decrease in trimaran resistance results in reducing fuel consumption compared to an equivalent monohull.

In recent decades, much research has considered the advantages of the trimaran concept. When the literature on trimarans is examined in general, it is clear that the most important parameter in resistance optimization is configuring the outriggers because of the flow-interference effect between the center-hull and outriggers (Yildiz et al., 2020).

*Corresponding author's email: kutama@na.its.ac.id, Tel.: +62-31-5964182, Fax.: +62-31-5964182
doi: 10.14716/ijtech.v12i3.4659

Optimum placement of these will result in an interaction between the wave train produced by the center-hull and the wave trains produced by the outriggers that ideally counteract each other at primary speed(s) of interest (Chen et al., 2016).

Preliminary research on trimarans was carried out by Gray (2003). In this study, resistance characteristics of a trimaran hull form with different arrangements were investigated to verify the theoretical prediction by comparing towing test results. The CFD method was utilized by Javanmardi et al. (2008) to analyze the hydrodynamic performance of the trimaran hull form with small-sized outriggers to determine optimum outrigger positions for minimum wave resistance performance. They also considered the wave interactions between the center-hull and outriggers to predict total wave-making resistance.

Shahid and Huang (2011) investigated the prediction of wave resistance on trimaran hull forms using CFD software. Three different mesh sizes and two different turbulence models were used to investigate the effect of mesh structure and turbulence models on the prediction of the resistance. CFD analyses were realized corresponding to Froude number ranges from 0.14 to 0.75, and the results were compared with the experimental data. Son (2015) performed CFD computations of a systematic series of trimaran hull forms. The center-hull form of the trimaran was developed based on the National Physical Laboratory (NPL) systematic series of round bilge hulls, and the sidehulls were created by scaling the center-hull to one-third size. Poundra et al. (2017) explained that the placement of the sidehull greatly affects ship resistance, both longitudinally and transversely. Catamaran hull interference can reduce resistance, as discussed by Iqbal and Samuel (2017) and Utama et al. (2021). This interference phenomenon also occurs in a more complex form on trimaran ships. The interaction between the hulls on a trimaran ship is examined by Sun et al. (2020), who prove that the flow field between the mainhull and sidehull of the trimaran can be captured by numerical calculations and PIV tests of the microscopic and macroscopic structures of the flow field. Trimaran configurations with proper positions can reduce residual resistance values (Heidari et al., 2019, Yanuar et al., 2020; Yildiz et al., 2020).

Further, the development of hull optimalization was carried out using the axe-bow. It uses straight vertical sides to dampen waves from the bow, which can result in a smooth pitching motion. Basically, the axe-bow in the extended section is empty space. The study of the axe-bow shows an increase in efficiency and a reduction in pitch acceleration because ships with axe-bows have less resistance in conventional models and reduce fuel use (Gelling, 2006).

The axe-bow developed by Damen Shipyard has better efficiency as well as better head-sea performance, with less slamming and higher speeds (Buckley, 2010). Damen Shipyard (2012) made a delivery of the first ship with an axe-bow, the Patrol Boat. The ship exhibits effective movement behavior and significantly lower drag while sailing. This provides a 20% reduction in fuel use and, consequently, fewer emissions. Through the CFD analysis of the optimum hull, it was possible to confirm the reduction of added resistance by the reflected wave around the bow smoothly spread to the side (Seok et al., 2019).

Two advantages to reducing ship resistance using the trimaran hull and the axe-bow have been mentioned in the previous literature. This paper discusses a combination of the two to obtain a better resistance reduction.

The main objective of the study is to analyze the resistance characteristics on a trimaran configuration with and without an axe-bow at the mainhull by utilizing the CFD method based on Reynolds-averaged Navier-Stokes (RANS) and an experimental model test using an ITTC standard towing tank (ITTC, 2011). Further, the interference effect was calculated to determine the best configuration.

2. Methods

2.1. Trimaran Model

The investigation used an NPL4a model with and without an axe-bow, as shown in Figures 1 and 2, and the principal particular can be seen in Table 1.

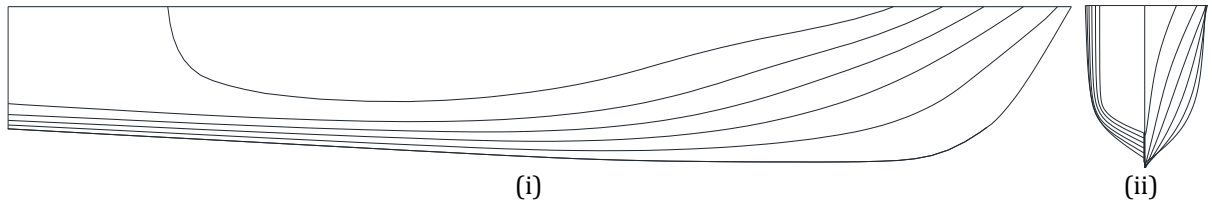

Figure 1 Mainhull NPL 4a: (i) Buttock plan; (ii) Body plan

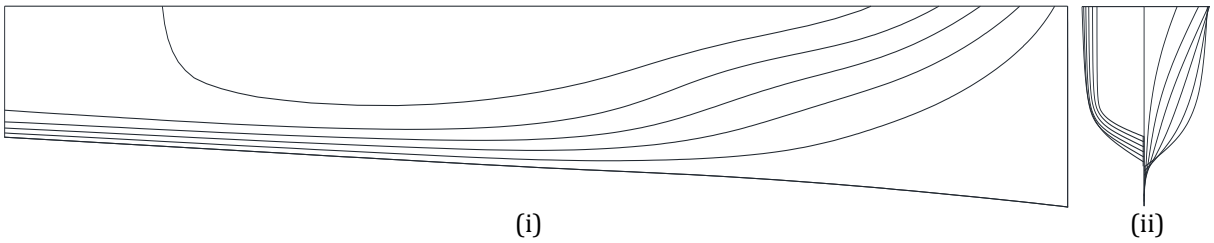

Figure 2 Mainhull NPL 4a with Axe-bow: (i) Buttock plan; (ii) Body plan

Table 1 Principal particular of the model

Parameter	Unit	Mainhull NPL 4a	Mainhull with Axe-bow	Sidehull NPL 4a
L_{OA}	m	1.252	1.252	1.058
L_{WL}	m	1.218	1.252	0.990
B	m	0.168	0.168	0.096
T	m	0.067	0.096	0.058
Wetted Surface Area	m^2	0.170	0.190	0.114
Displacement	kg	3.119	3.119	1.560
Block Coefficient (C_B)		0.397	0.194	0.397

2.2. Prediction of Trimaran Resistance

The enhanced design features of a trimaran lead to reducing the residual resistance; however, the consequence is a new form of resistance: the close positioning of the separate hulls leads to an interaction in both the total resistance.

This means that the following may be constructed. Consider a hull of beam B split into two equivalent hulls, each having a beam of B/2 and mainhull. The total resistance for the trimaran individual hull, namely R_T, divided into two equal resistances, namely $R_{TSidehull}$ and $R_{Tmainhull}$, is formulated in Equation 1:

$$R_T = R_{TMainhull} + 2R_{TSidehull} \quad (1)$$

As mentioned, the interaction of the waves is due to the position of the various hulls with reference to separation, implying that if the hulls are positioned so that there is no interaction between them, then no interference resistance would be experienced 10. By investigating the variations in separation, this interference resistance can be reduced. Interestingly, although interference would cause the hull to be inefficient, there are some positions where the interference produces favorable situations and the complete vessel experiences less resistance than the addition of the individual hulls acting separately. The total resistance of a trimaran can be calculated such that in Equation 2:

$$R_{TTrimaran} = R_{TMainhull} + 2R_{TSidehull} + \Delta R_T \quad (2)$$

where ΔR_T is the interference resistance due to the sidehull effect.

The computational fluid dynamics (CFD) technique, of varying degrees of complexity, may be used to predict various resistance components. The method would provide some insight into the pressure form drag. Full RANS codes may be used to predict the flow where separation and circulation occur, thus potentially providing good estimates of the form factor and possible scale effect. However, these methods are extremely computationally intensive, particularly for the high computation of Reynolds number flow (ANSYS, 2020).

The choice of turbulence models is found to be crucial in the simulation of wake fields. The turbulence model used in the current study is the SST (Shear Stress Transport) model developed by Menter et al. (2003), which has been used and validated by several researchers, including the work done by Bardina et al. (1997) with successful results. The viscous flow field is solved using the RANS solver implemented in ANSYS CFX, together with the use of continuity, turbulence k-ω and turbulence-SST equations.

2.3. Computational Fluid Dynamics

2.3.1. Numerical domain

The domain dimensions and boundary conditions are specified in Figure 3. The boundary conditions are specified as follows: the hull body is a no-slip condition that is imposed on the hull surface; the free-slip condition is applied to the top, side, and bottom walls; the symmetry condition is used for the hull center plane; the flow velocity at the inlet is defined as the tested speed; at the outlet, the hydrostatic pressure defined as a function of water-level height is applied; furthermore, the initial location of the free surface is determined by defining the volume-fraction function of water and air at the inlet and outlet.

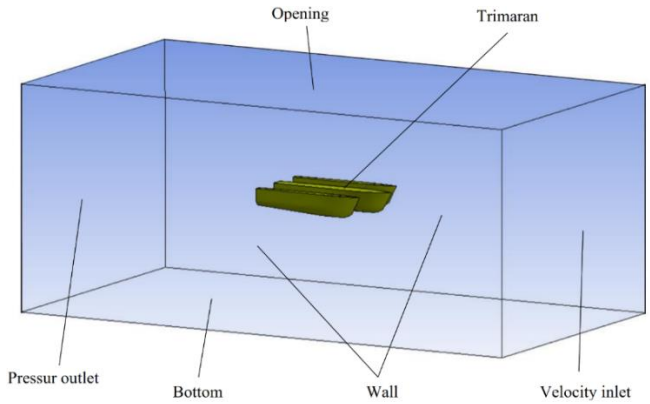

Figure 3 Boundary conditions

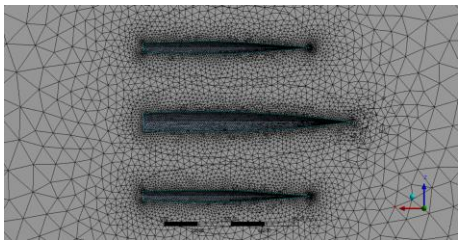

(a) Trimaran hull

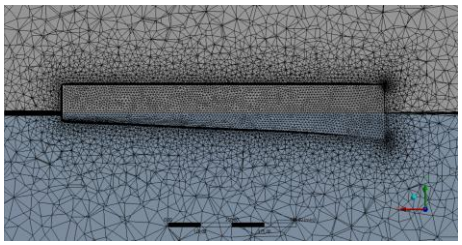

(b) Mainhull with axe-bow

Figure 4 Unstructured mesh with inflation

2.3.2. Grid independence

The mesh generation in this study was accomplished using Design Modeler. The calculation domain was discretized using structured and unstructured meshes. Considering the complex geometrical characteristics of the hull, a mesh with triangular elements is generated on the hull surface, and the boundary layer is refined with prism elements created through extending the surface mesh node. The region around the boat is filled with

tetrahedral elements with inflation, while in the far field, an unstructured mesh with grid generation is generated to reduce the number of elements, as shown in Figure 4.

The mesh size plays an important role in the calculation procedure. A fine mesh can always bring credible results in ANSYS CFX but at the same time increases the computational cost and time consumption due to the large element number. Therefore, to determine the mesh size with acceptable numerical accuracy and element number, mesh-convergence studies are carried out for the trimaran model of the NPL hull with S/L=0.3 at a Froude number of 0.4. The grid independence study is shown in Table 2 and Figure 5, according to Chung (2010); the number of elements used is about 1,583,256.

Table 2 Grid independence study

Total Element (×1000)	192	398	823	1,583	2,876
Resistance Total Coefficient (C_T) ($\times 10^{-3}$)	13.365	9.6136	8.1033	7.2356	7.1153
Difference (%)		28.07	15.71	10.71	1.66

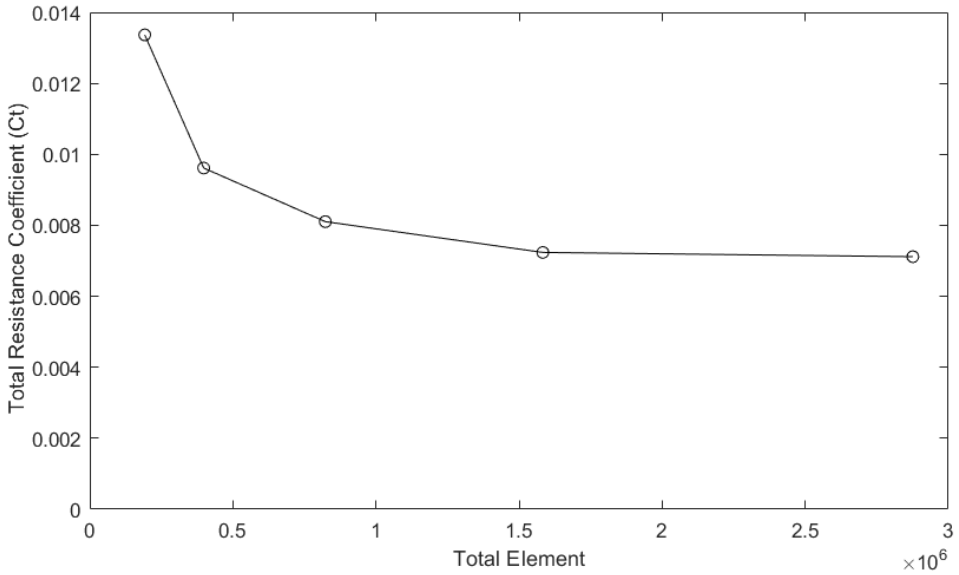

Figure 5 Grid Independence

Convergence studies of parameters are performed following a systematic refinement process to create multiple solutions. The numerical uncertainty of the CFD model utilizes the data in Table 2. In this paper, Richardson's extrapolation method for grid convergence could be a proper choice for estimating the mesh error (Zingg, 2012). The grid convergence study was conducted based on the ITTC uncertainty analysis recommendation (ITTC, 1999). The convergence study was made based on three varying mesh resolutions, which were categorized into coarse, medium, and fine mesh. The mesh was varied by modifying the face sizing while keeping the body sizing with a constant element size. The inflation layer was kept constant throughout the analysis, as the mesh resolution was based on the standard wall calculation, as shown in Table 3.

Table 3 Three varying mesh resolution details

Detail	Fine (1)	Medium (2)	Coarse (3)
Body sizing (m)	0.2	0.2	0.2
Face sizing (m)	0.01	0.02	0.04
Number of Elements (NE)	2,876,328	1,583,265	823,189
Drag coefficient ($\times 10^{-3}$) (C_T)	7.1153	7.2356	8.1033

The process is the same for time or any other study parameter. As for the refinement ratio r_i, the recommended value is $\sqrt{2}$, since the value is large enough to be sensitive to parameter changes and small enough to generate at least three successive solutions maintaining. A larger refinement ratio may be used; however, the mesh value has to be at least three. Based on formulas in the used equation section, outcomes have been calculated and presented at Table 4.

Table 4 The uncertainty analysis performed for the Trimaran model of NPL hull with S/L=0.3

Outcome	Equation	Value
Difference of estimation	$\varepsilon_{21}=NE_2/NE_1$	1.8169
	$\varepsilon_{32}=NE_3/NE_2$	1.9230
Refinement ratio	$r_{21}=C_{T2}-C_{T1}$	0.1203
	$r_{32}=C_{T3}-C_{T2}$	0.8677
Convergence	$R_i=\varepsilon_{21}/\varepsilon_{32}$	0.1386
Order of accuracy	$p=\ln(\varepsilon_{21}/\varepsilon_{32})/\ln(r_i)$	3.3090
Extrapolated relative error	$e_{21=}\varepsilon_{21}/r_i^p-1$	0.0523
	$e_{32}=\varepsilon_{32}/r_i^p-1$	0.3216
Grid convergence index (GCI)	$GCI_{21}=Fs\|e_{21}\|$	0.0029
	$GCI_{32=}Fs\|e_{32}\|$	0.0154

Convergence conditions of this system must first be clarified in order to assess the extrapolated value from the equations above. The convergence conditions are as follows:

1. Monotonic convergence: $0 < Ri < 1$
2. Oscillatory convergence: $Ri < 1$
3. Divergence: $Ri > 1$

For monotonic convergence, a generalized Richardson extrapolation is applied to estimate the errors and uncertainties. For oscillatory convergence, the results exhibit some oscillations. Lastly, for divergence, the results diverge, while errors and uncertainties are impossible to determine.

The grid convergence index (GCI) is a standardized way to report grid-convergence quality. It is calculated at refinement steps. Thus, we calculated a GCI for steps from grids 3 to 2, and from 2 to 1, where e is the error between the two grids and Fs is the safety factor (Fs=1.25).

The drag coefficient was converged based on the graphs, which proved that the mesh converged with different fineness of mesh. However, the fine mesh was still chosen for analysis as it provides a higher accuracy to the stimulation, which hence minimizes the error of investigation.

2.4. Experiment

The test-model creation procedure followed ITTC recommendations 7.5-02-05-01 (ITTC, 2002). The size of this winged ship test model adjusts the size of the towing tank test facility at the ITS Hydrodynamic Laboratory with a length of 50 m, a width of 3 m, and a depth of 2 m. The maximum towing carriage speed is 4.0 m/s. The mass density of the water towing tank is 999.1 kg/m^3, and the mass density of the air is about 1.164 kg/m^3 (for temperatures of 28^{o}C).

The test model is attached to the towing carriage through the towing guide (see Figure 6) with the setup that the test model can only move heaving and pitching freely and cannot move yawing or swaying so that no rolling or heeling moments arise.

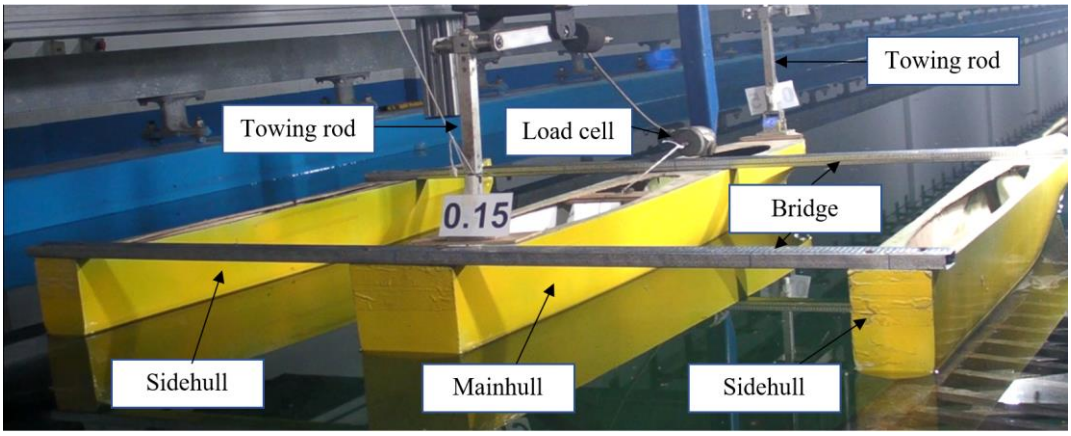

Figure 6 Experimental set-up of Trimaran model

The trim meter was installed in an upright position at the front and rear of the test model in a position that did not interfere with the towing guide. The test model was installed with the center line of the model. The instrumentation cable was laid in such a way that, at the time of measurement, it did not interfere with the motion of the test model.

3. Results and Discussion

3.1. Effect of the Axe-bow

A comparison of the calculation of resistance for conventional NPL 4a hull and NPL 4a with the axe-bow is presented. Experimental and CFD calculations show positive results due to the attachment of the axe-bow, as shown in Figure 7. Experimental calculations show that there is an average drag reduction of 11.5%, where the NPL hull with the axe-bow has a lower value than the conventional NPL 4a hull. This is also found in the calculation using the CFD approach, where there is a reduction in total absorption by 10.7%, which shows that the NPL 4a hull with the axe-bow has less resistance than the conventional NPL 4a hull. The positive effect of using the axe-bow was also reported by Romadhoni and Utama (2015), where the use of the axe-bow on a monohull ship was able to reduce resistance by 8–20%, whereas Bouckaert (2012) confirmed that the use of the axe-bow can reduce drag up to 10% when compared to conventional forms.

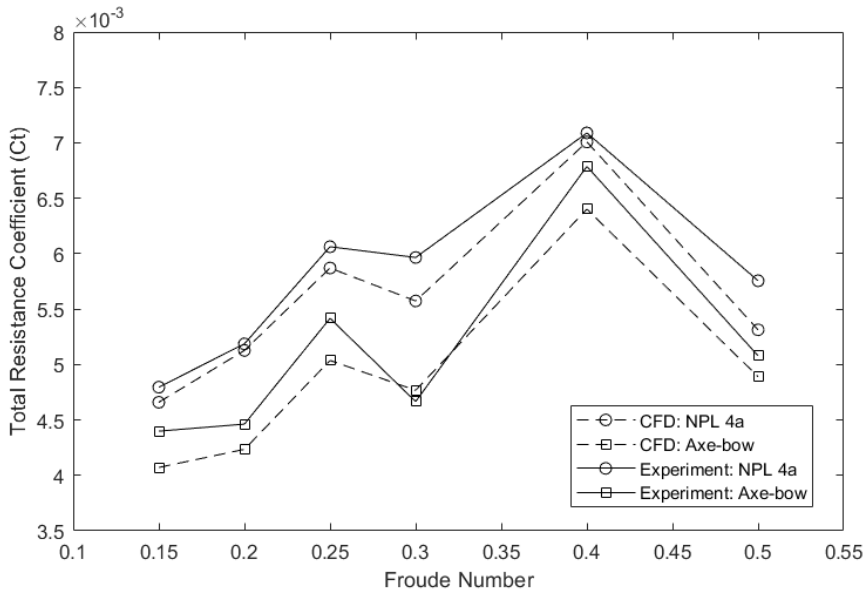

Figure 7 Comparison between CFD and experiment of mainhull

Furthermore, the fluid interaction with the hull is also influenced by the bow section of the ship, where in the presence of the axe-bow, fluid interactions tend to produce fewer waves at the front of the bow, as shown in Figure 8. The CFD simulation shows that it is quite clear that the bow with a conventional shape forms more waves when compared to the axe-bow shape. This impacts the resulting obstacles; namely, the conventional form of the hull has a larger barrier than the hull of the NPL with the axe-bow.

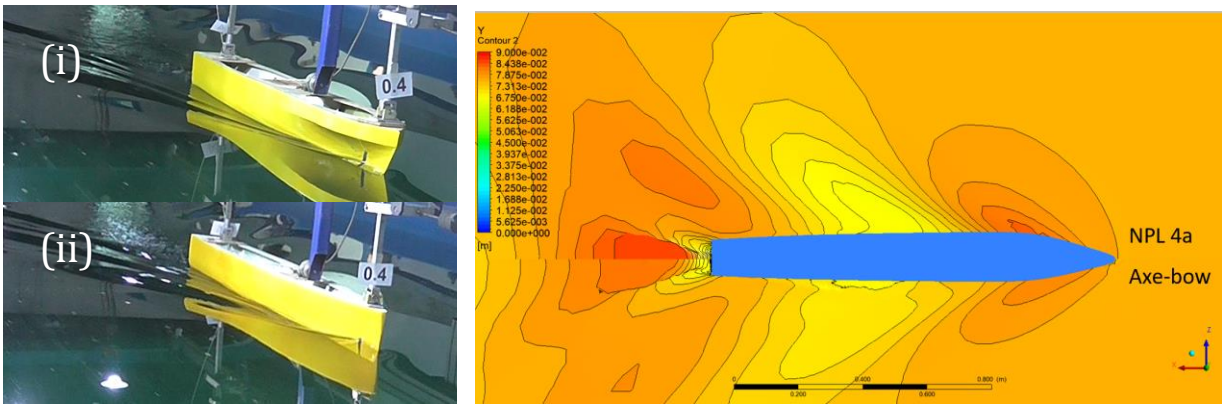

(a) (b)

Figure 8 (a) Experiment with wave-making of mainhull at Fn=0.4 , (i) NPL 4a, (ii) NPL 4a with axe-bow; (b) CFD simulation of NPL 4a with and without axe-bow

3.2. Hull Interaction

Calculating trimaran ship resistance was carried out using two approaches, namely CFD simulation and the towing tank experiment. The CFD simulation results are shown in Figure 8, where the conventional NPL 4a model has the same resistance trend as the axe-bow model. The individual trimaran model has about 5.6% smaller resistance compared to the trimaran ship resistance, with S/L = 0.3 and S/L = 0.4. This shows that there is interference between the hulls, which results in additional resistance.

Calculating trimaran ship resistance was also carried out using the model testing in the towing tank shown in Figure 9. The physical test results show that trimaran ships with variants S/L = 0.3 and 0.4 show greater results (about 6.5%) than the experimental results of individual trimaran ships. The physical test of the trimaran vessel showed hull interference, which resulted in increased drag.

The results of CFD calculations and experiments show that there are differences in the resistance to using the NPL 4a with the axe-bow, which is about 1%–8.4% smaller than the use of conventional hulls.

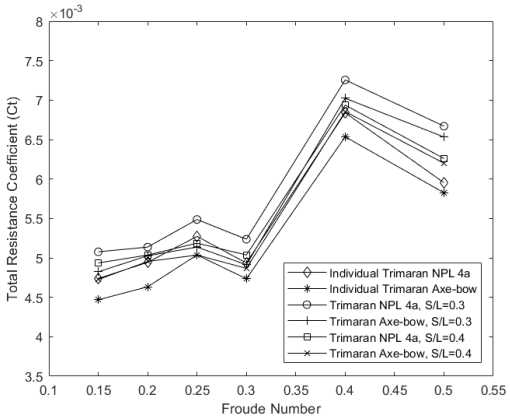

Figure 9 CFD Simulation for the Trimaran model

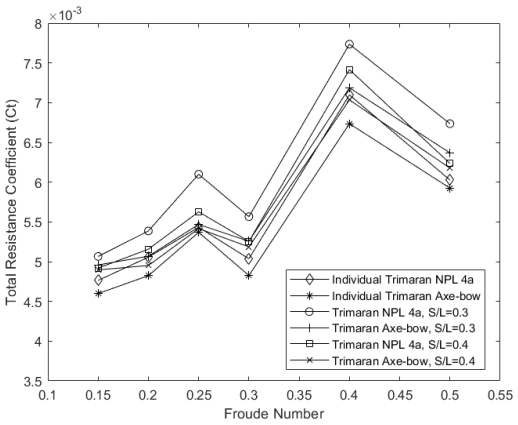

Figure 10 Experiment for Trimaran model

The interaction effect between the trimaran hull in the transverse direction (S/L) is very influential on the trimaran ship resistance. Figure 10 shows the calculation of the trimaran vessel hull on the NPL 4a hull with and without the axe-bow. The calculation of the total drag coefficient (C_T) for without interference (individual trimaran) has the smallest results compared to other trimaran variations. This shows that the interaction between the trimaran hulls gives rise to additional interference inhibition; in this case, total resistance interference by the trimaran hull.

Trimaran hull interference is an interaction caused by water between the hulls. This causes additional drag on the trimaran ship. Trimaran hull interference can be calculated using Equation 3:

$$\text{IF} = \frac{\Delta C_T}{C_T^{(M)}} \tag{3}$$

where IF is the interference factor of the trimaran and ΔC_T is the difference between the trimaran resistance coefficient ($C_{TTrimaran}$) and the trimaran resistance coefficient without interference or the sum of each individual hull $\left(C_T^{(M)} = C_{TMainhull} + 2C_{TSidehull}\right)$.

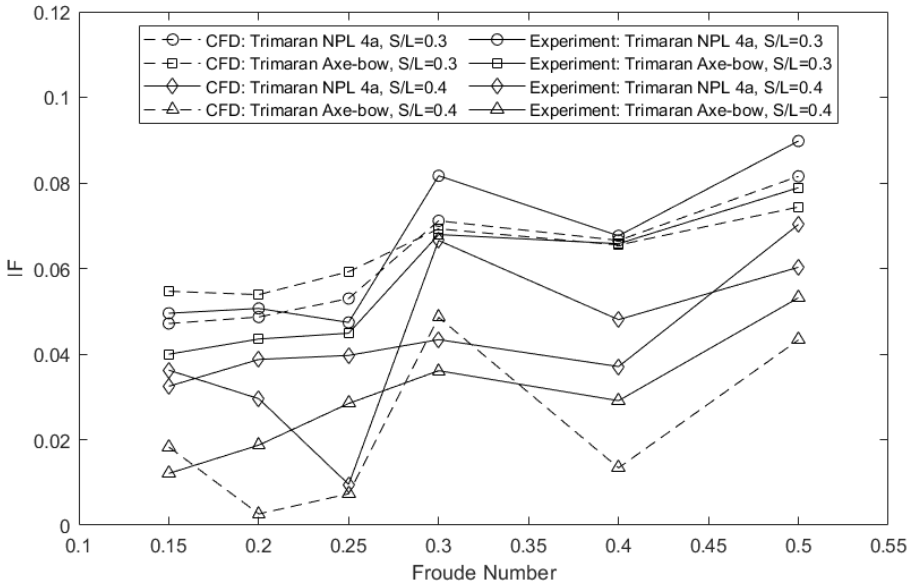

Figure 11 Interference of the Trimaran

The occurrence of wave-breaking around the hull makes this assumption an underestimate in the calculation of the wave-resistance component. Measuring wave-breaking directly is very difficult; hence, this can be observed only visually. Wave-breaking occurs in the front of the hull (bow), and interference occurs in the middle hull. Interference is influenced by the S/L distance, where the smaller the S/L distance, the greater the interference will occur, as shown in Figure 11. The existence of the axe-bow had a positive effect on trimaran hull interference, where there was a reduction of between 1.4%–8.4%. This occurred because there was a damping of the wave-making due to the axe-bow shape on the bow, as shown in Figure 13.

The interference that occurs between the trimaran hull models is in the form of waves and viscous interference. Interference that occurs can be well-visualized in the CFD simulation. Figure 14 shows the speed contours of the trimaran model with the NPL 4a hull (Figure 14a) and the NPL4a with the axe-bow (Figure 14b).

Flow-velocity contours indicate the effect of using a bow shape. In the conventional model, the flow in the bow has quite a few interactions; as a result, the flow interaction with

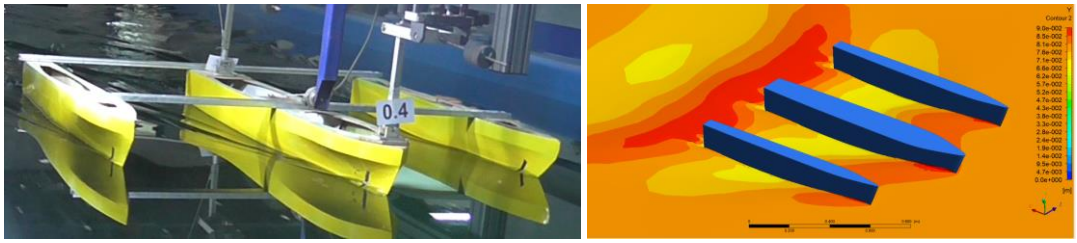

(a) Experiment (b) CFD simulation

Figure 12 Wave elevation of Trimaran with NPL hull at Fr=0.4 for S/L=0.4

(a) Experiment (b) CFD simulation

Figure 13 Wave elevation of Trimaran with axe-bow at Fr=0.4 for S/L=0.4

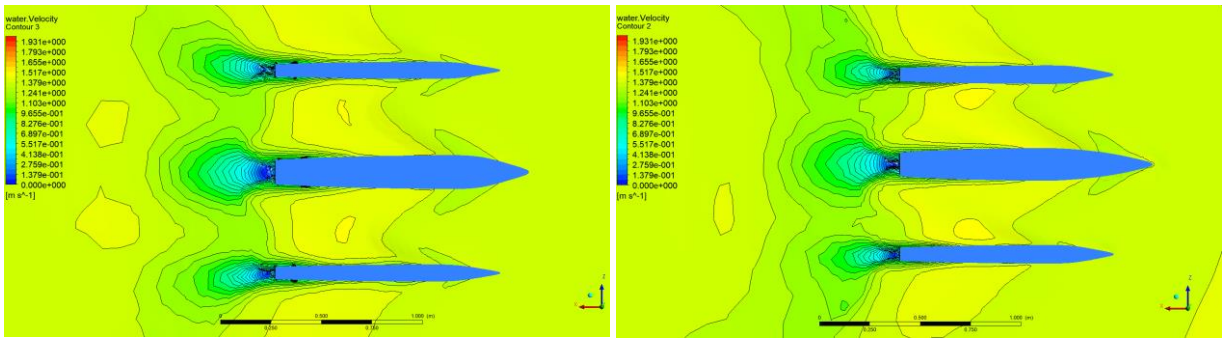

(a) NPL 4a (b) NPL4a with axe-bow

Figure 14 Velocity distribution of Trimaran at Fr=0.4 with S/L=0.4 for mainhull

the hulls increase afterward, causing an addition of the trimaran model to the absorption. Conversely, in the presence of the axe-bow, there is an interaction of fluid flow with more bow models; as a result, the interaction of water and the hull after is less and can reduce the resistance of the trimaran model.

4. Conclusions

An investigation into the effect of using the axe-bow on the resistance reduction of the trimaran configuration has been carried out numerically using the CFD approach and experimentally using an ITTC standard towing tank. The study was conducted using an NPL 4a model with and without the axe-bow on both the monohull and trimaran models with variations of S/L = 0.3 and 0.4. The use of CFD makes a very good contribution in relation to the calculation of resistance on monohull and trimaran vessels, both for NPL 4a and NPL 4a with the axe-bow. These results have been verified using experimental data with a discrepancy of about 2.7% on the monohull to 3.4% on the trimaran mode. Using the axe-bow gave a positive contribution, a reduction of up to 11.5% when compared to conventional hulls. Drag reduction of the ship is the ability of the axe-bow to reduce wave-

making due to the interaction of the bow and water. In the trimaran mode with variations of S/L = 0.3 and 0.4, the mainhull with the axe-bow was able to contribute to the reduction of resistance of up to 8.4%. This reduction in resistance occurs due to the contribution of the axe-bow, which can reduce wave-making in the bow, which further reduces the hull interaction.

Acknowledgements

The authors wish to thank the Directorate of Research and Community Services (DRPM) ITS for financing the research under a research scheme called "Postgraduate Research Grant" with contract number 920/PKS/ITS/2020. The authors also thank Mr. Langgeng Condro and Mr. Rudie Aminudin from the ITS Laboratory of Hydrodynamics for their help in the experimental test of the trimaran resistance.

References

ANSYS, 2020. *ANSYS CFX-Solver Theory Guide*. Ansys Inc, Canonsburg, PA, USA

Bardina, J.E., Huang, P.G., Coakley, T.J., 1997. Turbulence Modeling Validation, Testing, and Development. *NASA Technology Memorandum*

Bouckaert, B., 2012. Damen Shipyard's First Full Axe-bow Patrol Vessel Delivered to Cape Verdean Coast Guard. *Offshore Energy*, pp.1–7

Buckley, T., 2010. The Axe Factor: Damen & Amels Take a Bow. *The Yacht Report*, issue 111

Chen, Y., Yang, L., Xie, Y., Yu, S., 2016. The Research on Characteristic Parameters and Resistance Chart of Operation and Maintenance Trimaran in the Sea. *Polish Maritime Research*, Volume 23(s1), pp. 20–24

Chung, T.J., 2010. *Computational Fluid Dynamics*. UK: McGrawhill Inc. Cambridge University Press, Cambridge

Damen Shipyard, 2012. *Damen Shipyard's First Full Axe-bow Patrol Vessel Delivered to Cape Verdean Coast Guard*. Offshore Energy, Available Online at https://www.offshore-energy.biz/damen-shipyards-first-full-axe-bow-patrol-vessel-delivered-to-cape-verdean-coast-guard/

Elcin, Z., 2003. *Wave Making Resistance Characteristics of Trimaran Hulls*. Master's Thesis, Naval Postgraduate School, Canada

Gelling, J.L., 2006. The Axe Bow: The Shape of Ships to Come. *In:* International HISWA Symposium on Yacht Design and Yacht Construction, 19th. Amsterdam, the Netherlands

Gray, A.W., 2003. *A Preliminary Study of Trimarans*. West Virginia University

Heidari, M., Razaviyan, Z., Yusof, F., Mohammadian, E., Alias, A., Akhbari, M.H., Akbari, A., Movahedi, F., 2019. Numerical Analysis of Side Hull Configuration in Trimaran. *Revista Internacional de Métodos Numéricos para Cálculo y Diseño en Ingeniería.* Volume 35(2), pp. 1–17

Iqbal, M., Samuel, S., 2017. Traditional Catamaran Hull Form Configurations that Reduce Total Resistance. *International Journal of Technology*, Volume 8(1), pp. 85–93

ITTC, 1999. CFD Verification. *ITTC – Recommendation Procedure Guidelin*e. pp. 485–487

ITTC, 2002. *ITTC – Recommended Procedures Testing and Extrapolation Methods Resistance Test.* International Towing Tank Conference, pp. 1–11

ITTC, 2011. *ITTC – Recommended Procedures and Guidelines – Resistance Test (7.5-02-02-01)*. International Towing Tank Conference. Volume 13, pp. 1–13

Javanmardi, M., Jahanbakhsh, E., Seif, M., Sayyaadi, H., 2008. Hydrodynamic Analysis of Trimaran Vessels. *Polish Maritime Research*. Volume 15, pp. 11–18

Menter, F.R., Kuntz, M., Langtry, R., 2003. Ten Years of Industrial Experience with the SST Turbulence Model. *Turbulence Heat and Mass Transfer*, Volume 4, pp. 625–632

Poundra, G.A.P., Utama, I.K.A.P., Hardianto, D., Suwasono, B., 2017. Optimizing Trimaran Yacht Hull Configuration based on Resistance and Seakeeping Criteria. *Procedia Engineering*, Volume 194, pp. 112–119

Sulistyawati, W., Suranto, P., 2020. Achieving Drag Reduction with Hullform Improvement in Different Optimizing Methods. *International Journal of Technology*, Volume 11(7), pp. 1370–1379

Romadhoni, R., Utama, I.K.A.P., 2015. Analisa Pengaruh Bentuk Lambung Axe Bow Pada Kapal High Speed Craft Terhadap Hambatan Total (*Total Resistance Analysis of Axe-Bow Effect on High-Speed Craft*). *Kapal: Jurnal Ilmu Pengetahuan dan Teknologi Kelautan (Kapal: Journal of Marine Science and Technology)*, Volume 12(2), pp. 78–87

Seok, W., Kim, G.H., Seo, J., Rhee, S.H., 2019. Application of the Design of Experiments and Computational Fluid Dynamics to Bow Design Improvement. *Journal of Marine Science and Engineering*, Volume 7(7), pp. 1–13

Shahid, M., Huang, D., 2011. Resistance Calculations of Trimaran Hull Form using Computational Fluid Dynamics. *In:* Proceedings – 4th International Joint Conference on Computational Sciences and Optimization, CSO, Kunming and Lijiang City, China

Son, C.H., 2015. *CFD Investigation of Resistance of High-Speed Trimaran Hull Forms*. Master's Thesis, Graduate Program, Florida Institute of Technology Melbourne, Florida

Sun, C., Guo, C., Wang, C., Wang, L., Lin, J., 2020. Numerical and Experimental Study of Flow Field between the Main Hull and Demi-Hull of a Trimaran. *Journal Marine Science and Engineering*, Volume 8(12), pp. 1–18

Utama, I.K.A.P., Aryawan, W.D., Nasirudin, A., Sutiyo, Y., 2021. Numerical Investigation into the Pressure and Flow Velocity Distributions of a Slender-Body Catamaran Due to Viscous Interference Effects. *International Journal of Technology*, Volume 12(1), pp. 149–162

Yanuar, Y., Gunawan, G., Ibadurrahman, I., Mufti, R.R., Putro, J.W., 2020. Total Hull Resistance of Asymmetrical Trimaran Model with Hull Separation and Staggered Hull Variation of Sidehull. *AIP Conference Proceedings,* Volume 2255(1), p. 070006

Yildiz, B., Sener, B., Duman, S., Datla, R., 2020. A Numerical and Experimental Study on the Outrigger Positioning of a Trimaran Hull in Terms of Resistance. *Ocean Engineering*. Volume 198, pp. 106938

Zingg, D., 2012. Viscous Airfoil Computations using Richardson Extrapolation. *In:* 10th Computational Fluid Dynamics Conference, Honolulu, USA